AIP Applied Physics Letters

In situ observation of nickel as an oxidizable electrode material for the solid-electrolyte-based resistive random access memory

Jun Sun, Qi Liu, Hongwei Xie, Xing Wu, Feng Xu et al.

Citation: Appl. Phys. Lett. **102**, 053502 (2013); doi: 10.1063/1.4790837
View online: http://dx.doi.org/10.1063/1.4790837
View Table of Contents: http://apl.aip.org/resource/1/APPLAB/v102/i5
Published by the AIP Publishing LLC.

Additional information on Appl. Phys. Lett.

Journal Homepage: http://apl.aip.org/
Journal Information: http://apl.aip.org/about/about_the_journal
Top downloads: http://apl.aip.org/features/most_downloaded
Information for Authors: http://apl.aip.org/authors

ADVERTISEMENT

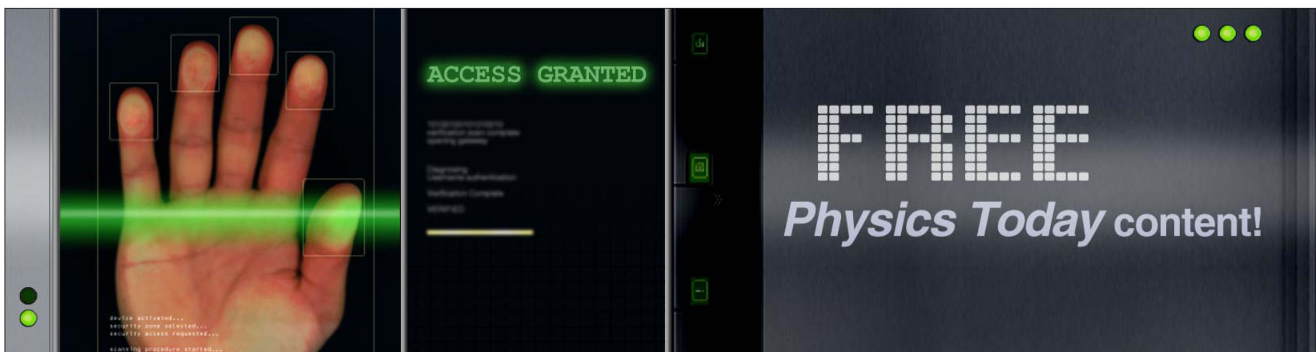

Downloaded 09 Jul 2013 to 223.3.54.19. This article is copyrighted as indicated in the abstract. Reuse of AIP content is subject to the terms at: http://apl.aip.org/about/rights_and_permissions

CrossMark click for updates

In situ observation of nickel as an oxidizable electrode material for the solid-electrolyte-based resistive random access memory

Jun Sun,[1,a)] Qi Liu,[2,a)] Hongwei Xie,[2] Xing Wu,[1] Feng Xu,[1] Tao Xu,[1] Shibing Long,[2] Hangbing Lv,[2] Yingtao Li,[2] Litao Sun,[1,b)] and Ming Liu[2]
[1]*SEU-FEI Nano-Pico Center, Key Laboratory of MEMS of Ministry of Education, Southeast University, Nanjing 210096, China*
[2]*Laboratory of Nano-fabrication and Novel Devices Integrated Technology, Institute of Microelectronics, Chinese Academy of Sciences, Beijing 100029, China*

(Received 16 December 2012; accepted 25 January 2013; published online 5 February 2013)

In this letter, we dynamically investigate the resistive switching characteristics and physical mechanism of the Ni/ZrO_2/Pt device. The device shows stable bipolar resistive switching behaviors after forming process, which is similar to the Ag/ZrO_2/Pt and Cu/ZrO_2/Pt devices. Using *in situ* transmission electron microscopy, we observe in real time that several conductive filaments are formed across the ZrO_2 layer between Ni and Pt electrodes after forming. Energy-dispersive X-ray spectroscopy results confirm that Ni is the main composition of the conductive filaments. The ON-state resistance increases with increasing temperature, exhibiting the feature of metallic conduction. In addition, the calculated resistance temperature coefficient is equal to that of the 10–30 nm diameter Ni nanowire, further indicating that the nanoscale Ni conductive bridge is the physical origin of the observed conductive filaments. The resistive switching characteristics and the conductive filament's component of Ni/ZrO_2/Pt device are consistent with the characteristics of the typical solid-electrolyte-based resistive random access memory. Therefore, aside from Cu and Ag, Ni can also be used as an oxidizable electrode material for resistive random access memory applications. © *2013 American Institute of Physics*. [http://dx.doi.org/10.1063/1.4790837]

Solid-electrolyte-based *resistive random-access memory* (RRAM), also known as conductive bridging memory or programmable metallization cell, has been extensively studied in recent years as a promising nonvolatile memory technology because of its excellent scalability, high density, and superior memory performances.[1,2] The device consists of a solid electrolyte layer sandwiched between an oxidizable electrode and an inert counter electrode, and its resistance switching is related to the formation/annihilation of conductive filaments (CFs) inside the solid electrolyte layer.[1] The CFs involve the metal ions transferring from the oxidizable electrode to the counter electrode through the electrochemical metallization effect.[1,2] Up to now, many materials have been explored as switching layer for the solid-electrolyte-based RRAM application, including Cu/Ag compound (e.g., CuS,[3] AgS,[4] AgGeSe,[5] and CuC (Ref. 6)), binary oxides (e.g., Ta_2O_5,[7] ZrO_2,[8–10] HfO_2,[11] SiO_2,[12] and ZnO (Ref. 13)), organic materials,[14] and α-Si.[15] As another important functional material in RRAM, the oxidizable electrode materials, which supply metal ions into solid electrolyte layer to form CFs, have a significant effect on resistive switching performances. However, only few materials have been reported for this application except Ag and Cu.[3–15] Recently, Lin *et al.*[16] have found that Ni/HfO_2/Pt device shows a similar nonpolar resistive switching behavior to Cu/HfO_2/Pt device and the content of Ni inside HfO_2 film obviously increases after electroforming. Based on these results, they suggested that Ni is a possible oxidizable electrode material for solid-electrolyte-based RRAM application. If the role of Ni as an oxidizable electrode can be confirmed, Ni will be a worthy oxidizable electrode material candidate for solid-electrolyte-based RRAM application due to its full compatibility with the current CMOS technology.[17] However, direct experimental evidence confirming the role of Ni electrode in the solid-electrolyte-based RRAM system is insufficient.

In this study, *in situ* transmission electron microscopy (TEM) observation directly confirms that the bipolar resistive switching in Ni/ZrO_2/Pt devices originates from the formation and dissolution of CFs. Energy-dispersive X-ray spectroscopy (EDS) analysis and temperature-dependent switching characteristics reveal that Ni conductive bridge is the physical origin of CFs. Based on these experimental results, the microscopic resistive switching process between the high resistance state (HRS or OFF-state) and low resistance state (LRS or ON-state) is discussed to elucidate the role of Ni electrode in RRAM.

Two types of Ni/ZrO_2/Pt devices are, respectively, prepared on the platform of a W probe and a SiO_2/Si substrate by successively depositing a 10 nm thick Ti adhesion layer, a 50 nm-thick Pt bottom electrode layer, a 40 nm thick ZrO_2 film, and a 70 nm Ni top electrode layer using electron beam evaporation. The evaporation process is performed at room temperature, with the chamber pressure maintained at $\sim 1 \times 10^{-5}$ Pa. The Ni/ZrO_2/Pt devices on the SiO_2/Si substrate with $100 \times 100\,\mu m^2$ cell area are fabricated by the lithography and lift-off processes. The device structure is shown in the inset of Fig. 1(a). The Ni/ZrO_2/Pt stacked films on the platform of the W probe are fabricated to multiple TEM specimens with small lateral sizes (~200 nm) by using a dual-beam focused ion beam (FIB) system (FEI Nov 200 nanolab).

a)J. Sun and Q. Liu contributed equally to this work.
b)Author to whom correspondence should be addressed. Electronic mail: slt@seu.edu.cn. Tel.: +86-25-83792632-8813. Fax: +86-25-83792939.

 © 2013 American Institute of Physics

Downloaded 09 Jul 2013 to 223.3.54.19. This article is copyrighted as indicated in the abstract. Reuse of AIP content is subject to the terms at: http://apl.aip.org/about/rights_and_permissions

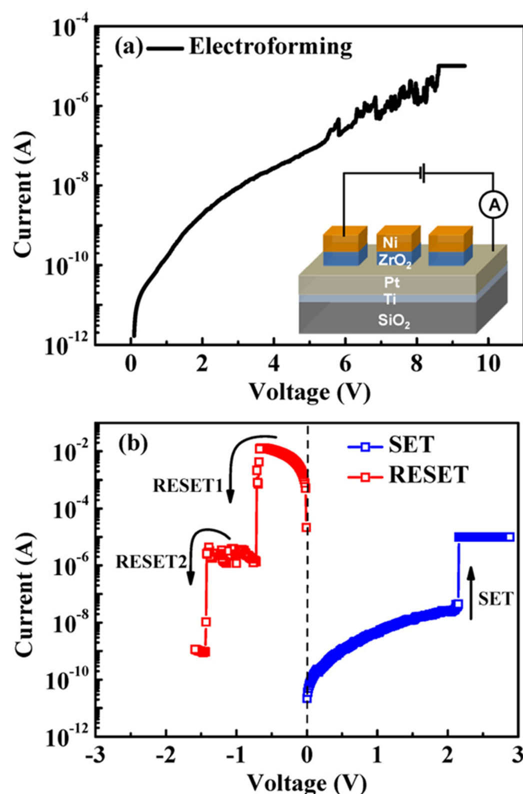

FIG. 1. (a) Typical electroforming process and (b) bipolar resistive switching behavior of $Ni/ZrO_2/Pt$ device. The inset of (a) shows a schematic diagram of the device structure and measurement setup.

The detailed fabrication process of the TEM specimens is described elsewhere.[18] The $Ni/ZrO_2/Pt$ devices on the SiO_2/Si substrate are used to study the resistive switching characteristics under different ambient temperatures, and the TEM specimens are used to achieve real-time visualization of the nanoscale structural changes with high spatial resolution inside TEM under applied electrical bias.

Figure 1 shows the typical I-V characteristics of the $Ni/ZrO_2/Pt$ devices, in which electric measurements are performed by using an Agilent B1500 semiconductor device analyzer and bias polarity is defined with reference to the bottom Pt electrode. The schematic diagrams of the $Ni/ZrO_2/Pt$ device structure and the electrical measurement setup are shown in the inset of Fig. 1(a). The initial state of the fresh devices is HRS with a resistance of $\sim 10^{10}$ Ω at 0.1 V read voltage. To trigger repeatable resistive switching behavior in the fresh $Ni/ZrO_2/Pt$ device, an electrical forming process with high voltage is required. As shown in Fig. 1(a), the device current suddenly increases at $\sim$9 V when a positive voltage is first applied to the Ni electrode with a 10 μA compliance current (I_{CC}), indicating the device switches from the initial state to the LRS. It is worth noting that the forming process is difficult to achieve under a negative voltage sweep. After the positive electroforming process, the $Ni/ZrO_2/Pt$ device shows a stable bipolar resistive switching behavior (Fig. 1(b)). The switching processes from the HRS to LRS and from the LRS to HRS are defined as SET and RESET processes, respectively. When a positive voltage with 10 μA I_{CC} applied to the Ni electrode, the current of the device rapidly increases and the device switches from the HRS to LRS at the SET voltage (V_{SET}). Under reversal voltage, the device suddenly transits back to the HRS at the RESET voltage (V_{RESET}). The RESET process often shows the stepwise current transition, implying that the switching behavior is dominated by the formation and rupture of multiple CFs.[10] The typical resistances of the LRS and HRS at 0.1 V are on the order of 10^2 and 10^9 Ω, respectively. The ratio between these two states can be more than 10^6. This switching behavior of the $Ni/ZrO_2/Pt$ device is similar to that of typical solid-electrolyte-based RRAM devices, such as $Ag/ZrO_2/Pt$,[9] $Cu/ZrO_2/Pt$,[19] $Cu/Ta_2O_5/Pt$,[7] and Ag/ZnO/Pt.[13]

Dedicated *in situ* TEM analysis is performed on the $Ni/ZrO_2/Pt$ TEM specimens to understand the microscopic mechanism of resistive switching in the $Ni/ZrO_2/Pt$ device. Figure 2(a) shows the schematic sketch of the *in situ* TEM experimental setup. A Nanofactory Instruments STM-TEM holder is used for *in situ* manipulation and electrical measurement. The holder contains a fixed and a movable contacting terminal. In the *in situ* TEM characterization, the W probe with the $Ni/ZrO_2/Pt$ TEM specimens and another W probe with a sharp-tip are installed at the fixed and movable contacting terminals of the holder, respectively. During the electrical testing, the TEM specimen is connected by the two W probes, and the voltage is applied to the fixed contacting terminal while the movable terminal is grounded. The current density of electron beam used in the HRTEM observation is about 10 A/cm^2. The current density is difficult to damage the observational materials because it is far lower than those experiments, where e-beam is used for *in situ* drilling and welding (10^5–10^6 A/cm^2).[20,21] Furthermore, the result of electron irradiation with long time also confirms that the impaction of the observing current on the device materials is negligible. None of the micro-structure changes are observed when the stack RRAM films are exposed to long time ($\sim$1 h) electron irradiation with $\sim$10 A/cm^2 current density.

Figure 2(b) shows a typical cross-section TEM image of a fresh $Ni/ZrO_2/Pt$ device, which exhibits the Ni, ZrO_2, and

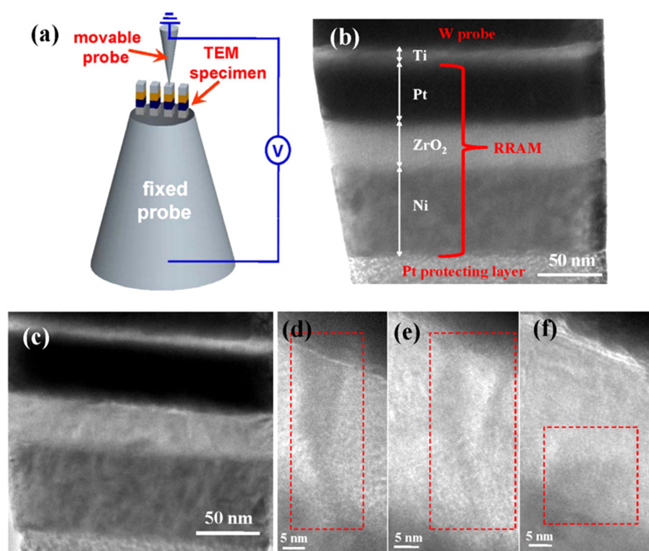

FIG. 2. (a) Schematic of the *in situ* TEM experimental setup. (b) Cross-sectional TEM micrograph of a fresh $Ni/ZrO_2/Pt$ device. (c) Cross-sectional TEM micrograph of the device after the electroforming process. Some nanoscale dark-regions inside ZrO_2 film appear after forming. (d) and (e) show the enlarged TEM images of these nanoscale dark-regions.

Downloaded 09 Jul 2013 to 223.3.54.19. This article is copyrighted as indicated in the abstract. Reuse of AIP content is subject to the terms at: http://apl.aip.org/about/rights_and_permissions

Pt triple-stacked films with clear interface. The fresh TEM specimens are generally in the HRS. Then, when a positive voltage with 100 nA I_{CC} is applied to the Ni electrode, the device transits from the initial OFF-state to the ON-state (the data are not shown here). After the forming process, some nanoscale dark-regions appear inside the ZrO_2 layer, as can be seen from Fig. 2(c). By enlarging these dark-regions, several complete CFs can be clearly observed to connect the Ni electrode with the Pt electrode across the ZrO_2 layer (Figs. 2(d) and 2(e)). The results directly confirm that the formation and dissolution of multiple CFs dominate the resistive switching phenomena in the Ni/ZrO_2/Pt devices. It is noted that the multiple CFs is not formed/dissolved at the same time.[10,18] In addition, an incomplete CF connected to the Ni electrode is observed inside the ZrO_2 layers (Fig. 2(f)), implying that the CF starts to nucleate and grow from the active Ni electrode to Pt electrode. The number and shape of the CFs observed in the Ni/ZrO_2/Pt device are similar to those in the Ag/ZrO_2/Pt and Cu/ZrO_2/Pt devices in our previous study.[18]

To verify the chemical composition of the CF, the EDS composition analysis is carried out in scanning TEM (STEM) mode. As shown in Fig. 3, the signal of Ni element is detected in the CF region (circular region labeled by "1" in the inset of Fig. 3(a)), while no Ni signal is detected outside the CF region (circular region labeled by "2" in the inset of Fig. 3(a)). The result indicates that Ni is the primary elemental component of the nanoscale CF in our Ni/ZrO_2/Pt device.

As demonstrated in the previous work,[8,13] the value of resistance temperature coefficient (α) can also give a clue to clarify the physical nature of the CFs. Figure 4 shows the ON-state resistance (R_{ON}) as a function of temperature in the range of 313 K to 398 K. As shown in Fig. 4, R_{ON} increases linearly with increasing temperature, which is a typical electronic transport behavior in metals. The temperature dependence of metallic resistance can be written as $R(T) = R_0\ [1 + \alpha(T - T_0)]$, where R_0 is the resistance at temperature T_0 and α is the resistance temperature coefficient.[8] Thus, the resistance temperature coefficient of the Ni/ZrO_2/Pt device in the ON-state can be calculated as $\alpha = 1.41 \times 10^{-3}\ K^{-1}$ (inset of Fig. 4). Moreover, the value of the resistance temperature coefficient ranges from $1.27 \times 10^{-3}\ K^{-1}$ to $2.20 \times 10^{-3}\ K^{-1}$, with an average value of $1.80 \times 10^{-3}\ K^{-1}$ for ten Ni/ZrO_2/Pt devices. The results match excellently with the resistance temperature coefficient of the Ni nanowire with 10–30 nm diameter,[22,23] indicating that the metallic behavior of the ON-state originates from the conducting Ni filaments with the size around tens of nanometers.

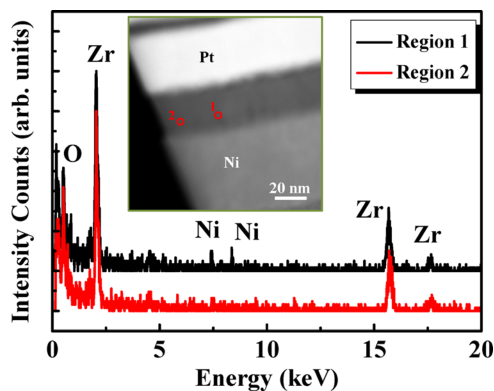

FIG. 3. EDX spectrums of the ON-state device collected at two locations as indicated in the insetted STEM micrograph. Compared to the region away from filament (marked as "2"), Ni signal is obviously observed in the filament region (marked as "1").

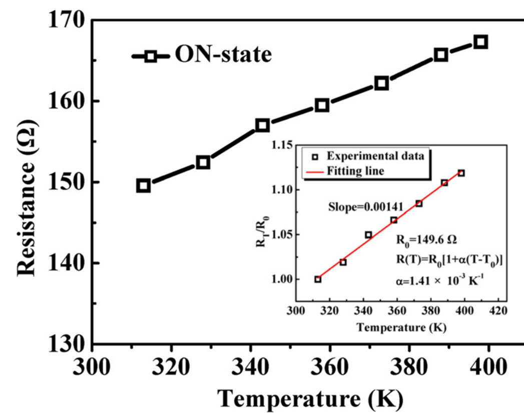

FIG. 4. Temperature dependence of the ON-state resistance of the Ni/ZrO_2/Pt device. The inset shows that the resistance temperature coefficient (α) of the ON-state device is $1.41 \times 10^{-3}\ K^{-1}$.

Through the above analysis, we are able to give a microscopic scenario to describe the bipolar resistive switching phenomenon in the Ni/ZrO_2/Pt devices. When a positive voltage is applied to the Ni electrode, the nanoscale conductive Ni filaments are formed in the ZrO_2 layer under the electrochemical metallization effect, leading to that the resistance of the device drops abruptly and the device switches to the ON-state. Under the reversal voltage, the rupture of Ni filament primarily occurs at the weakest part due to the electrochemical effect assisted by Joule heating.[8] As a result, the device switches back to the OFF-state because the current in this case can only transport through the insulated ZrO_2 film. The current study clearly demonstrates that the electrical switching characteristics and physical mechanism of the Ni/ZrO_2/Pt device are consistent with those of the typical solid-electrolyte-based RRAM.[1,2,18,24] Therefore, Ni can be used as an effective oxidizable electrode material for solid-electrolyte-based RRAM devices.

In conclusion, we directly demonstrate that multiple CFs are formed across the ZrO_2 layer between the Ni and Pt electrodes inside Ni/ZrO_2/Pt device after forming process by *in situ* TEM observation. Based on EDS analysis and temperature-dependent switching characterization, we confirm that the observed CFs consist of metallic Ni atoms as a result of the Ni electrochemical reactions. This dynamic investigation clearly demonstrates that Ni can be used as an effective oxidizable electrode material for the solid-electrolyte-based RRAM applications, which will greatly enrich the materials system and can help to achieve high-performance RRAM.

The authors thank K. W. Peng from NCNST for the help of TEM sample preparation. This work was funded by the Ministry of Science and Technology of China under Grant Nos. 2009CB623702, 2011CB707601, 2011AA010401, 2011CBA00602, 2010CB934200, 2011CB921804, 2009CB930803, and 2011AA010402 and NSFC under Grant Nos. 61274114, 51071044, 21243011, 61106055, 61221004,

Downloaded 09 Jul 2013 to 223.3.54.19. This article is copyrighted as indicated in the abstract. Reuse of AIP content is subject to the terms at: http://apl.aip.org/about/rights_and_permissions

60825403, 61106119, 61106082, 50972160, and Gatan Scholarship for Excellence in Science.

[1]R. Waser, R. Dittmann, G. Staikov, and K. Szot, Adv. Mater. **21**, 2632 (2009).
[2]T. Hasegawa, K. Terabe, T. Tsuruoka, and M. Aono, Adv. Mater. **24**, 252 (2012).
[3]T. Sakamoto, H. Sunamura, H. Kawaura, T. Hasegawa, T. Nakayama, and M. Aono, Appl. Phys. Lett. **82**, 3032 (2003).
[4]Z. Xu, Y. Bando, W. Wang, X. Bai, and D. Golberg, ACS Nano **4**, 2515 (2010).
[5]L. Chen, Z. Liu, Y. Xia, K. Yin, L. Gao, and J. Yin, Appl. Phys. Lett. **94**, 162112 (2009).
[6]M. Pyun, H. Choi, J.-B. Park, D. Lee, M. Hasan, R. Dong, S.-J. Jung, J. Lee, D.-J. Seong, J. Yoon, and H. Hwang, Appl. Phys. Lett. **93**, 212907 (2008).
[7]T. Tsuruoka, K. Terabe, T. Hasegawa, and M. Aono, Nanotechnology **21**, 425205 (2010).
[8]W. Guan, M. Liu, S. Long, Q. Liu, and W. Wang, Appl. Phys. Lett. **93**, 223506 (2008).
[9]Q. Liu, S. Long, H. Lv, W. Wang, J. Niu, Z. Huo, J. Chen, and M. Liu, ACS Nano **4**, 6162 (2010).
[10]Q. Liu, C. Dou, Y. Wang, S. Long, W. Wang, M. Liu, M. Zhang, and J. Chen, Appl. Phys. Lett. **95**, 023501 (2009).
[11]Y. Wang, Q. Liu, S. Long, W. Wang, Q. Wang, M. Zhang, S. Zhang, Y. Li, Q. Zuo, J. Yang, and M. Liu, Nanotechnology **21**, 045202 (2010).
[12]C. Schindler, G. Staikov, and R. Waser, Appl. Phys. Lett. **94**, 072109 (2009).
[13]Y. C. Yang, F. Pan, Q. Liu, M. Liu, and F. Zeng, Nano Lett. **9**, 1636 (2009).
[14]B. Cho, J.-M. Yun, S. Song, Y. Ji, D.-Y. Kim, and T. Lee, Adv. Funct. Mater. **21**, 3976 (2011).
[15]Y. Yang, P. Gao, S. Gaba, T. Chang, X. Pan, and W. Lu, Nature Commun. **3**, 732 (2012).
[16]K.-L. Lin, T.-H. Hou, J. Shieh, J.-H. Lin, C.-T. Chou, and Y.-J. Lee, J. Appl. Phys. **109**, 084104 (2011).
[17]X. Li, W. H. Liu, N. Raghavan, M. Bosman, and K. L. Pey, Appl. Phys. Lett. **97**, 202904 (2010).
[18]Q. Liu, J. Sun, H. Lv, S. Long, K. Yin, N. Wan, Y. Li, L. Sun, and M. Liu, Adv. Mater. **24**, 1774 (2012).
[19]Q. Liu, S. Long, W. Wang, Q. Zuo, S. Zhang, J. Chen, and M. Liu, IEEE Electron Device Lett. **12**, 1335 (2009).
[20]R. F. Egerton, P. Li, and M. Malac, Micron **35**, 399 (2004).
[21]S. Y. Xu, M. L. Tian, J. G. Wang, J. Xu, J. M. Redwing, and M. H. W. Chan, Small **1**, 1221 (2005).
[22]E. Shapira, A. Tsukernik, and Y. Selzer, Nanotechnology **18**, 485703 (2007).
[23]Y. Rheem, C. M. Hangarter, E.-H. Yang, D.-Y. Park, N. V. Myung, and B. Yoo, IEEE Trans. Nanotechnol. **7**, 251 (2008).
[24]X. Wu, K. Li, N. Raghavan, M. Bosman, Q. X. Wang, D. Cha, X. X. Zhang, and K. L. Pey, Appl. Phys. Lett. **99**, 093502 (2011).

Downloaded 09 Jul 2013 to 223.3.54.19. This article is copyrighted as indicated in the abstract. Reuse of AIP content is subject to the terms at: http://apl.aip.org/about/rights_and_permissions